Wave Reflections and Velocities Generated by Detonation Propagation Through Circular Arcs

Scott I. Jackson, David J. Lont, Josue Martinez
Department of Aerospace Engineering
Texas A&M University
College Station, TX USA

Mark Short
Shock and Detonation Physics Group
Los Alamos National Laboratory
Los Alamos, NM, USA

1 Introduction

Detonation propagation confined by an arc or annular channel is currently an active area of research [1–5] with application to rotating detonation engine combustors. The detonation wave dynamics under curved confinement have also been shown to affect the stability of the detonation front [5]. Detonation propagation confined by an arc or annular channel of constant curvature diffracts at the inner radius and reflects from the wall at the outer radius, which may cause the wave to intersect with the outer wall at a non-normal angle. Under these circumstances, the incident detonation will deflect the postshock flow towards the wall and wave reflections must be generated to return the flow parallel to the wall. The reflected wave generated is coincident with the lead shock at the wall for this *regular reflection* mode. Regular reflections will exist when both the incident and reflected wave can satisfy the oblique shock relations, which is generally possible when the wave angle between the lead detonation and the upstream wall is significantly less than perpendicular. However, no regular reflection solution may be possible for wave angles approaching normal. Under these circumstances, a small normal detonation wave or reactive *Mach stem* will be generated at the wall instead, which will branch into an incident detonation and reflected shock wave a short distance from the wall to form a *Mach reflection*. The detonation wave may also exhibit *negative curvature* by curving upstream [5].

For reactive flow under these conditions, the detonation shape, speed, and reflected mode can be coupled. The confinement imposes a global curvature on the detonation shock, which modifies its shape and velocity. The reflected wave mode is influenced by both this shock shape at the outer wall and the gas equation of state, which will evolve through the wave for reactive flow. Finally, the detonation shape and velocity can be further affected by a region of this reacting flow termed the detonation driving zone (DDZ) [3, 4]. Kasahara and collaborators [1, 2, 6] were able to generate nearly constant angular detonation velocities when the confiner curvature was large relative to the detonation cell width and used this effect to establish a Detonation Shock Dynamics relation for the several gas mixtures studied. Short et al. [5] examined this effect numerically and found that, for fixed inner radius, the modes of wave reflection would vary with increasing outer radius. Smaller outer radii generated nearly planar and cellularly

Correspondence to: sij@tamu.edu

unstable waves, but increasing outer radii first created negatively curved waves (concave towards the upstream reactant flow), followed by Mach reflection, and finally regular reflection. Correspondingly, the global curvature induced on the wave also reduced the extent of the DDZ, eventually reducing it to a small region adjacent to the inner radius. Subsequent experimental work has also focused on the stability limits of the arc configuration [7], but there have been relatively few efforts on the reflected wave modes that occur in these systems [8]. The open-shutter imaging technique used by Kasahara [1] also did not definitively capture the types of reflection modes present.

This study reports the wave reflection modes and velocities generated by a detonation stabilized in an arc of constant curvature. The mixture pressure, inner radii, and outer radii of curvature are varied and the resulting detonation shape, reflection mode, and angular velocity are recorded using short-integration-time chemiluminescence imaging. Mixtures are chosen such that the cellular instability scales are small relative to the channel width.

2 Experimental

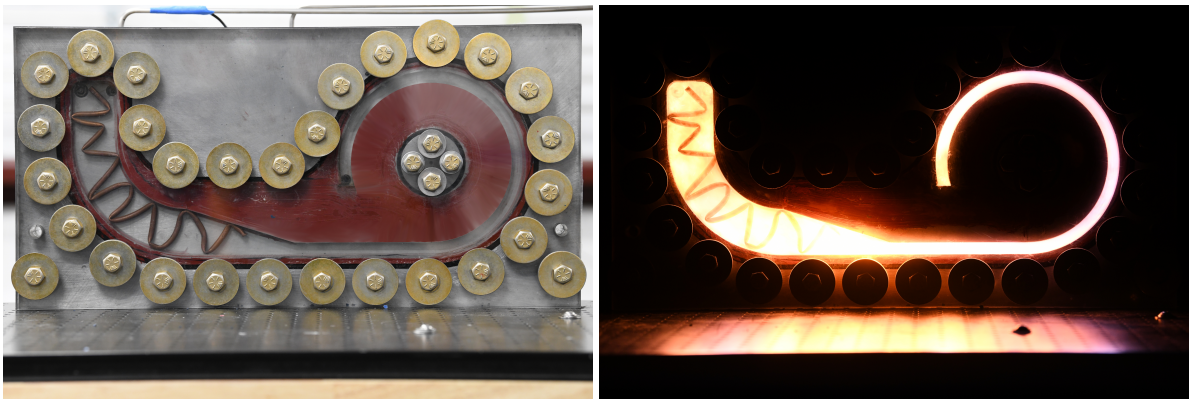

Figure 1: The experimental assembly (left) and long-exposure image of the combustion process (right) for the 87.3-mm inner radius and 100-mm outer radius configuration.

The experimental assembly is shown in Fig. 1. The design consisted of three layers: an aluminum back plate, an aluminum middle layer which makes up the arced channel of rectangular cross section, and a set of front plates made of polycarbonate for optical access. The back plate had three threaded holes: one for an automotive spark plug and two for gas handling feedthroughs that are located at the beginning and end of the channel. The middle layer contained removable inserts that were machined to contain a channel consisting of an ignition volume, a transition volume, and an arced channel. The removable inserts allowed the channel inner and outer radii to be varied.

The depth of the rectangular cross-section was 12.7 mm and constant throughout the channel. The ignition volume had a width of 50 mm and a length of approximately 200 mm. It also contained a length of coiled tubing which served as an obstacle to promote deflagration-to-detonation transition. The transition volume was 350 mm long, beginning with a width of 50 mm that then tapered to match the arc width (Fig. 1), which was an independent variable. The arc region spaned 270°, yielding arc lengths of 256 and 471 mm for radii of 50 and 100 mm, respectively. The inner radius was varied between 50 and 87.3 mm, while the outer radius was varied between 60, 80, and 100 mm with specific combinations listed in Table 1 below. Each plate in Fig. 1 was 305 mm wide and 610 mm long. Sealing was accomplished with O-rings along the perimeter of the channel and silicone sealant. Bolts along the channel perimeter fastened the assembly.

During an experiment, the channel was first evacuated using a vacuum pump. It was then filled with stoichiometric ethylene and oxygen mixtures using the method of partial pressures. Initial pressures tested ranged from 0.25–1.00 bar. The gases were mixed for several minutes after filling using a diaphragm pump. The spark ignition was generated via a coil-on-plug automotive ignition coil. The resulting combustion chemiluminescence was recorded with a Phantom v2640 framing camera. Two different imaging arrangements were utilized for each configuration. A lower resolution mode with high frame rates was used to measure detonation angular velocity through the arc. The frame rates varied from 33–50 kHz and yielded image resolutions of 1 px/mm. A higher resolution mode was also used to capture the wave structure at increased detail, yielding image resolutions up to 8 px/mm. In all cases, the image integration time was 142 ns.

Table 1: Summary of test configurations and results.

R_i (mm)	R_o (mm)	w (mm)	P_0 (bar)	ω (mrad/μsec)	D_i/D_{CJ}	D_{CJ} (mm/μs)	Mode
50.0	100.0	50.0	1.00	44.29±0.21	0.933	2.373	Regular
50.0	100.0	50.0	0.70	43.31±0.13	0.920	2.356	Regular
50.0	100.0	50.0	0.60	43.26±0.12	0.921	2349	Regular
50.0	100.0	50.0	0.50	43.04 ± 0.09	0.920	2.340	Regular
50.0	100.0	50.0	0.40	40.89±0.25	0.878	2.329	Regular
50.0	80.0	30.0	1.00	44.44±0.05	0.936	2.373	Regular
50.0	80.0	30.0	0.70	43.67±0.16	0.927	2.356	Regular
50.0	80.0	30.0	0.60	43.27±0.06	0.921	2349	Regular
50.0	80.0	30.0	0.50	42.69±0.04	0.906	2.356	Regular
50.0	80.0	30.0	0.40	42.27±0.25	0.907	2.329	Regular
50.0	60.0	10.0	1.00	44.20±0.06	0.931	2.373	Mach stem
50.0	60.0	10.0	0.90	–	–	–	Mach stem
50.0	60.0	10.0	0.80	–	–	–	Mach stem
50.0	60.0	10.0	0.70	43.82±0.06	0.930	2.356	Mach stem
50.0	60.0	10.0	0.60	42.92±0.05	0.914	2.349	Mach stem
50.0	60.0	10.0	0.50	42.39±0.01		2.356	Negative curvature
50.0	60.0	10.0	0.40	42.02±0.16		2.329	Negative curvature
87.3	100.0	12.7	1.00	–	–	–	Mach stem
87.3	100.0	12.7	0.90	–	–	–	Mach stem
87.3	100.0	12.7	0.80	–	–	–	Mach stem
87.3	100.0	12.7	0.70	–	–	–	Mach stem
87.3	100.0	12.7	0.60	42.39±0.02	0.948	2.349	Mach stem
87.3	100.0	12.7	0.50	41.84±0.02	0.939	2.340	Negative curvature
87.3	100.0	12.7	0.40	–	–	–	Negative curvature
87.3	100.0	12.7	0.30	–	–	–	Negative curvature
87.3	100.0	12.7	0.25	–	–	–	Near planar

3 Results

Figure 2 shows a series of successive high-speed imaging frames of the detonation propagating in a channel with a 50-mm inner radius and 100-mm outer radius at 0.5-bar initial pressure mixture. For brevity, channel configurations are referred to as ID/OD mm (e.g. 50/100 mm) below. The detonation entering the arc is near planar in frame (a) with a weak reflected shock train generated by the transition

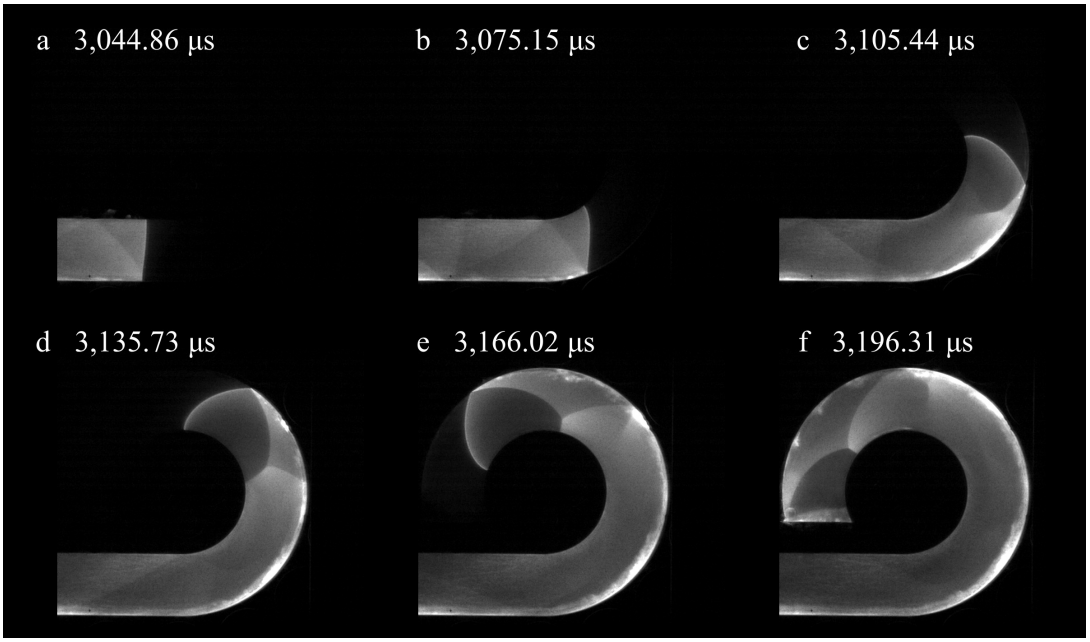

Figure 2: Wave evolution with the 50/100 mm arc at 0.50 bar with timing relative to spark ignition.

region. After entry into the arc (frame b), it diffracts at the inner radius and reflects from the outer radius (frame c). The wave reflections reshock the products and locally increase the luminosity. The resulting wave consists of a leading detonation wave with a regular shock reflection. The reflected wave forms a Mach stem at the inner radius for frames d-f. The detonation front and regular reflection qualitatively appear to form a constant shape within the first 90° of the arc, while the Mach stem at the second reflection continuously decreases in length with propagation. The detonation front also remains normal to the inner wall surface throughout the experiment. For this mixture, the detonation cell size is estimated to be 0.9 mm, which is not resolvable at the image resolution shown. However, high-resolution images do capture evidence of the cellular instability at the front for this test condition. After wave passage, the combustion products appear most luminous for late times at the outer radius of the arc as has been seen by other researchers [1, 2]. The cause of this feature is not known, but may be due to sealant decomposition or late ignition of small amounts of reactant initially trapped in the small (30 micron) gap between the window and metal substrate. Varying the pressure for this specific channel configuration does not change the wave dynamics (Fig. 3) for this configuration or for the 50/80 mm case, but does for others.

Figure 4 shows the evolution of the detonation front with increasing pressure for the 87.3/100 mm configuration. At the lowest pressure (0.25), the wave is near planar with no significant reflection and shows evidence of cellular instabilities on the front. As pressure is increased (0.30–0.6 bar), the outer radius of the wave becomes increasingly curved towards the reactants (negative curvature as discussed in [5]) and the reflected shocks increase in luminosity. A distinct Mach stem develops at the outer radius for pressures of 0.70–1.0 bar. A similar trend was also observed for the 50/60 mm outer radius configuration. Identification of Mach reflection relied on the presence of a discontinuous shock slope change at the triple point with the reflected wave coincident at that point. Negative curvature waves did not exhibit these features.

The summary of these observed wave reflection modes is shown in Table. 1. The numerical work of Short et al. [5] observed lead wave shape transitions from planar, to negatively curved, to a Mach stem and then to regular reflection at the outer radius when increasing the outer radius while holding the inner

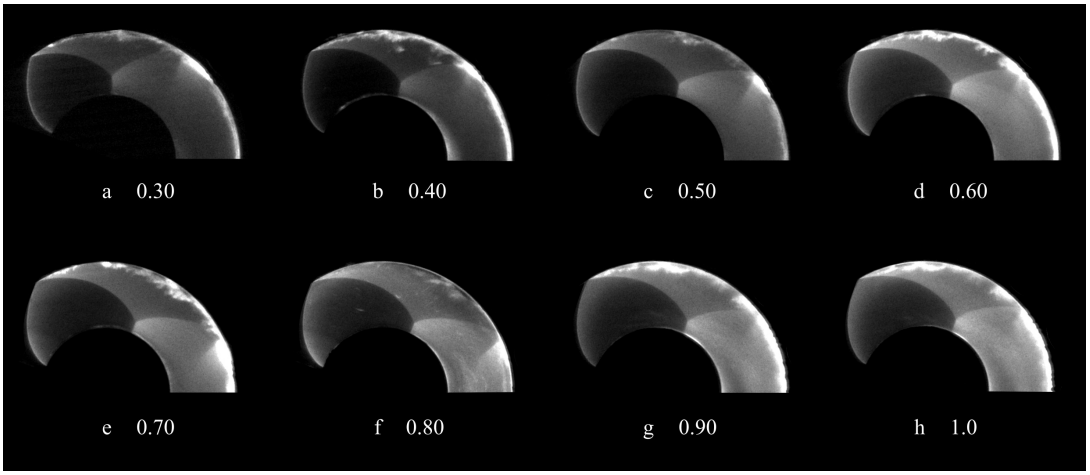

Figure 3: Wave variation with pressure (listed on the figure in bar) for the 50/100 mm case.

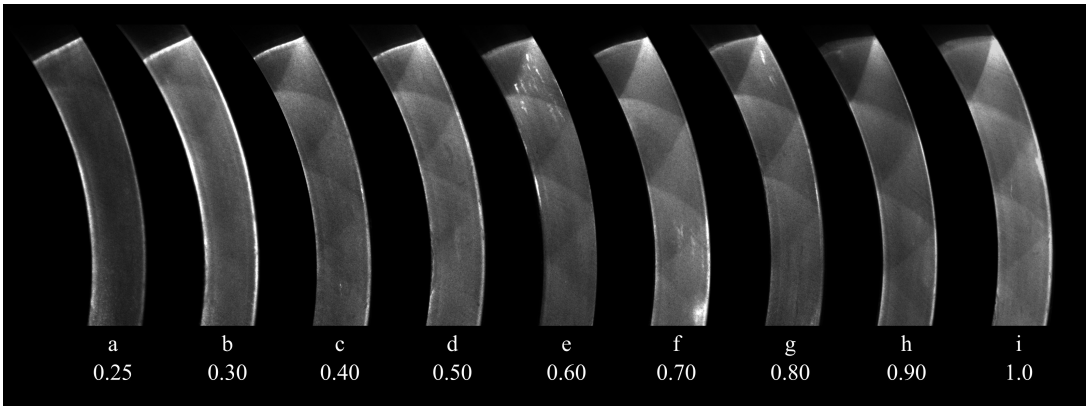

Figure 4: Wave variation with pressure (listed on the figure in bar) for the 87.3/100 mm case.

radius and pressure constant. Similar trends are seen in this experimental data, though the resolution is currently limited.

4 Wave Shapes and Angular Velocities

For selected tests, the lead shock position was manually identified to allow for determination of the detonation velocity and wave shape. Figure 5a shows the wave shapes from different timesteps plotted in cylindrical coordinates of radius r relative to the arc origin and azmuthial angle θ relative to the innermost portion of the wave for the 50/100 mm case at 0.5 bar. At early times, the wave shape is evolving as it adapts to the arced channel geometry, but reaches a quasisteady shape after traveling less than 90°. In general, the wave shape appears to become quasisteady after propagating an arc length equal to several channel widths, but still exhibits small variations as shown. These are possibly within the experimental uncertainty. The front shape versus pressure is also in Fig. 5b for the same configuration. For this case, the angular span of the wave increases with pressure, which may be correlated with increasing detonation velocity.

Angular wave speeds ω were also calculated for selected cases as a function of radius by fitting a line ($\theta[r] = \omega\, r + \theta_0$) to successive shock shapes in regions of steady wave shape. The average wave speed over all radii is shown in Table 1 with ranges that indicate the standard deviation of this mean.

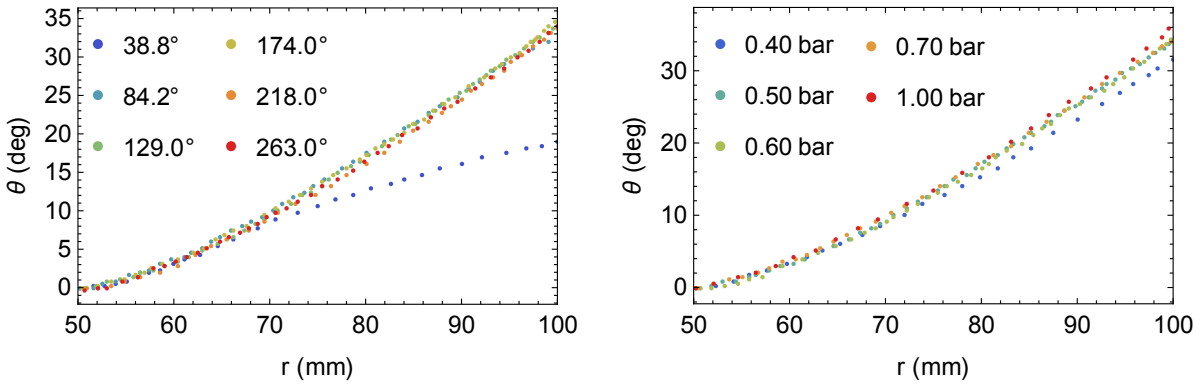

(a) Front variation with arc angle at 0.5 bar.

(b) Front shape evolution with initial pressure.

Figure 5: Front shapes for the 50/100 mm configuration.

The detonation velocity at the inner inner radius is also listed and normalized by the Chapman-Jouguet detonation velocity D_i/D_{CJ}. Both the angular wave speed and normalized detonation velocity increase with pressure for a given arc configuration. The wave speed dependence on radius is more complex and evaluation is ongoing.

References

[1] H. Nakayama, T. Moriya, J. Kasahara, A. Matsuo, Y. Sasamoto, and I. Funaki, "Stable detonation wave propagation in rectangular-cross-section curved channels," *Combustion and flame*, vol. 159, no. 2, pp. 859–869, 2012.

[2] H. Nakayama, J. Kasahara, A. Matsuo, and I. Funaki, "Front shock behavior of stable curved detonation waves in rectangular-cross-section curved channels," *Proceedings of the Combustion Institute*, vol. 34, no. 2, pp. 1939–1947, 2013.

[3] M. Short, J. Q. James, C. Meyer, and C. Chiquete, "Steady detonation propagation in a circular arc: a detonation shock dynamics model," *Journal of Fluid Mechanics*, vol. 807, pp. 87–134, 2016.

[4] M. Short, J. Quirk, and C. C. C. Meyer, "Detonation propagation in a circular arc: reactive burn modelling," *Journal of Fluid Mechanics*, vol. 835, pp. 970–998, 2018.

[5] M. Short, C. Chiquete, and J. Quirk, "Propagation of a stable gaseous detonation in a circular arc configuration," *Proceedings of the Combustion Institute*, vol. 37, no. 3, pp. 3593–3600, 2019.

[6] Y. Kudo, Y. Nagura, J. Kasahara, Y. Sasamoto, and A. Matsuo, "Oblique detonation waves stabilized in rectangular-cross-section bent tubes," *Proceedings of the Combustion Institute*, vol. 33, no. 2, pp. 2319–2326, 2011.

[7] R. Hencel, M. Fotia, and J. Hoke, "Propagation of gaseous detonations in high aspect ratio planar curved channels," in *International Colloquium on the Dynamics of Explosions and Reactive Systems*, Naples, Italy, June 19–24 2022.

[8] V. Rodriguez, C. Jourdain, P. Vidal, and R. Zitoun, "An experimental evidence of steadily-rotating overdriven detonation," *Combustion and Flame*, vol. 202, pp. 132–142, 2019.